The Incorporation of Hemin Catalysts and Alumina Nanoparticles in a Medium of *Spondias mombin* Leaf Extract of A Sulfonated Polysulfone-Polyaniline_Alumina Membrane Electrode Assembly for Fuel Cell Technologies

Armi Wulanawati[1, 2 *], Yoki Yulizar[1*], S. Mulijani[2], F. Rohman[3]

[1] Department of Chemistry, Faculty of Mathematics and Natural Sciences, Universitas Indonesia, Depok 16424, Indonesia

[2] Department of Chemistry, Faculty of Mathematics and Natural Sciences, IPB University, Bogor 16680, Indonesia

[3] Research Center of Energy Materials National Research and Inovation Agency (BRIN) , Tangerang Selatan 15314, Indonesia

** Corresponding Author. E-mail: armiwulanawati@apps.ipb.ac.id (A. Wulanawati), yokiy@sci.ui.ac.id (Y. Yulizar)*

Telp: +62-251-8624567, +62-21-7270027

Abstract

The development of sustainable Membrane Electrode Assembly (MEA) is crucial for advancing fuel cell technology. This study presents a novel MEA design that incorporates metal oxide nanoparticles synthesized using natural materials into a high performance membrane and employs a non-platinum catalyst. Specifically, alumina (Al_2O_3) nanoparticles were synthesized in medium *Spondias mombin* leaf extract, which served as both a base source and a capping agent. Alumina nanoparticles combined with polyaniline serve as a composite material to enhance the hydrophilicity, structural and thermal stability, power density, and proton conductivity of a sulfonated polysulfone-based composite membrane. Alumina is known as a catalyst support with a large surface area, while polyaniline is a conductive polymer that readily interacts with metal oxides and hemin, which is rich in electrons, exhibits catalytic activity. Based on the characterization of physical and

chemical properties, the SPSU-PANI_Al_2O_3 7.5% composite MEA using a hemin catalyst on the cathode in a fuel cell (DMFC) demonstrated good structural and thermal stability, low methanol permeabilitity (3,37 x 10^{-6} cm^2/detik), and high power density (90.76 mW/cm^2), but low proton conductivity. Furthermore, Electrochemical cell testing of the hemin catalyst, which identified two reduction peaks at 0.48-0.52 V and 1.22 V similar to those of the Pt catalyst at the cathode demonstrates that the hemin catalyst provides comparable cell potential and catalytic activity for the oxygen reduction reaction for fuel cell technologies.

Keywords:

Fuel Cell; Alumina Nanoparticles; Hemin Catalyst; Membrane Electrode Assembly, *Spondias mombin*

1. Introduction

The membrane electrode assembly (MEA) is a crucial component in fuel cells, such as direct methanol fuel cells (DMFC), consisting of a proton exchange membrane (PEM) in the form of a solid polymer electrolyte that conducts protons, and a catalyst layer. The most widely used polymer electrolyte membrane, as a PEM, is perfluorosulfonic acid (PFSA), also known as Nafion. This is because the Nafion membrane has high proton conductivity, namely 0.1 S/cm at room temperature [1], high electron insulation, as well as being durable and hydrophilic [2]. Many studies have been conducted in an effort to increase proton conductivity either through modification of the Nafion membrane or by designing other membranes from aromatic hydrocarbon-based polymers, including polysulfone [3,4], polyether ether ketone [5], as well as polystyrene [6].

Polysulfone (PSU) is among several aromatic polymers known to tend to dissolve in a variety of solvents (halogen derivatives, dimethyl acetamide, dimethyl sulfoxide), withstand high temperatures. Good tensile strength, a wide range of operating pH, and appropriate responsiveness in aromatic electrophilic substitution, such as sulfonation [7]. In general, after sulfonation, supporting materials are added to form composites [7]. The Functional group-modified additives improve PEM properties, namely, mechanical strength, proton conductivity, and chemical stability [8]. The formation of composite materials can be carried out using plant extracts

(roots/stems/leaves) that serve as a source of hydroxyl groups (-OH) and capping agents to enhance structure, smoothness, and homogeneity. One plant that can be used in synthesis with high phytochemical content, including tannins, saponins, alkaloids, flavonoids, and phenols, is *Spondias mombin* [9].

Several PEM in composite form have been produced, including a sulfonated polysulfone-polyaniline_Nb_2O_5 composite membrane (PSU-SPANI_Nb_2O_5) that makes a proton conductivity of 6.74 x 10^{-2} S/cm [10]. The relatively high proton conductivity of this composite membrane is due not only to the use of Nb_2O_5 as one of many transition metal oxides rich in active adsorption sites and interactions with water molecules, but also to the presence of polyaniline (PANI), which is among the conductive polymers widely used as sensors, electromagnetic interference shields, electronic devices, and energy storage devices [11]. Polymeric nanocomposites have attracted significant interest due to the enhancement of matrix properties that can result from the incorporation of a small quantity of nanostructures into the polymeric matrix [12]. According to Alhoshan et al. [13], Al_2O_3 is one type of metal oxide nanoparticle, alongside ZnO, SiO_2, CNT, MgO, and ZrO_2, that has been used as a filler to develop a matrix in composite membranes. In addition, Al_2O_3 meets the requirements as a catalyst support because it has inert properties, good thermal stability, can bind catalysts, and has a relatively large surface area and pores that are evenly dispersed.

Catalysts play a primary role to improve fuel cell performance, especially the oxygen reduction reaction (ORR) at the cathode, which is difficult. Therefore, a suitable catalyst is needed to accelerate ORR. Fe-N-C catalysts produced through pyrolysis with iron chloride, glycine, and acetylene black precursors show ORR catalytic activity with power density comparable to that of Pt-based catalysts [14]. Meanwhile, mixing Fe, N, and C precursors sourced respectively from Fe(II) lactate, glycine, and glucose produces a heme-like active site with increased catalytic activity [15]. Based on these considerations, and in an effort to enhance the performance of membrane fuel cells by focusing on cost-effective and environmentally sustainable components, this study introduces a novel Membrane Electrode Assembly (MEA) that integrates key innovations. The central novelty of this work lies in the systematic development of a sulfonated polysulfone (SPSU)-based composite membrane, where Al2O3 nanoparticles are produced via a green chemistry approach using Spondias mombin leaf extract. This unique membrane is paired with a hemin catalyst as a non-

platinum, high-potential alternative for the cathode. The core objective of this research is therefore to systematically fabricate, thoroughly characterize, and critically evaluate the electrochemical performance of the SPSU-PANI_Al_2O_3 composite MEA with a hemin catalyst in fuel cell technologies, aiming to establish the viability of this integrated, sustainable system as a high-performance substitute for conventional, expensive platinum-based MEA.

2. Materials and Methods

2.1 Materials

Spondias mombin leaves were obtained from IPB Biofarmaka Fields, Bogor, Indonesia. The leaves were identified at the Center for Research on Biosystematics and Evolution BRIN Cibinong-Bogor, polysulfone (Mn = 22.000), H_2SO_4, nitrogen gas, chloroform, dichloromethane, methanol, n-hexane, dimethyl acetamide, NaOH, HCl, phenolphthalein, Wagner's reagent, $FeCl_3$, acetic anhydride, aluminum nitrate hydrate, aniline, ammonium persulfate, carbon paper, platinum on carbon, Hemin on carbon and aquabidest.

2.2. Preparation of *Spondias mombin* leaf extract (SMLE)

Spondias mombin leaves are washed and dried. The dried leaves are ground into a fine powder using a blender. Next, the extraction process is carried out in two stages, namely maceration and fractionation. In the maceration stage, 50 g of *Spondias mombin* leaf powder is first placed in a beaker, then macerated with 250 mL of methanol solvent (leaf powder/solvent ratio of 1:5) for 7 days, with periodic stirring for 20 minutes daily. The mixture is then filtered and separated from the residue to obtain the methanol filtrate of *Spondias mombin* leaves. In the next stage, the methanol filtrate of *Spondias mombin* leaves was partitioned with n-hexane solvent (1:1). The results obtained were two fractions, namely, the methanol fraction and n-hexane fraction. The methanol fraction from the partitioning was then evaporated using a rotary vacuum evaporator at 55 °C until all the solvent was removed. The concentration resulted in a methanol fraction, to which 100 mL of distilled water was added, and this solution was then referred to as the *Spondias mombin* leaf extract stock solution (SMLE).

2.3. Synthesis of Al_2O_3 Nanoparticles

A total of 1.125 g of $Al(NO_3)_3 \cdot 9H_2O$ solid was dissolved in 100 mL of distilled water to obtain a 0.03 M $Al(NO_3)_3$ solution. In total, 50 mL of 0.03 M aluminum nitrate solution and *Spondias mombin leaf* extract were mixed in a precursor: extract volume ratio of 1:5. The mixture was stirred at 80 °C for 4 hours and then aged for 24 hours to complete the formation of the colloid. The colloid was separated and calcined at 600 °C for 12 hours. The Al_2O_3 nanoparticle powder was characterized using FTIR, TGA/DTA, XRD, PSA, SEM, SAED, TEM, and HRTEM.

2.4. Synthesis of Polyaniline (PANI)_Al_2O_3 Composite

A total of 3.0 mL of aniline was added dropwise to 100 mL of 1.5 M HCl solution and stirred constantly. A total of 0.0%, 3.0%, 7.5%, 10.0%, and 12.5% (w/w) Al_2O_3 was slowly added to the aniline solution. Meanwhile, the oxidant solution was prepared by adding 4.0 g of ammonium persulfate to 100 mL of 1.5 M HCl solution. The polymerization of aniline and the synthesis of PANI_Al_2O_3 composite were performed by adding the oxidant solution dropwise to the initial mixture at a temperature of 10 °C, while stirring constantly for 22 hours. The resulting greenish-black slurry was filtered and washed continuously with distilled water until the filtrate was colorless. The PANI_Al_2O_3 composite obtained was air-dried in an oven at 100 °C for 24 hours. Next, 0.9 g of the composite was mixed with 50 mL of 0.1 M NaOH and stirred for 5 hours. It was then filtered and rewashed with 75 mL of 0.1 M NaOH and 75 mL of distilled water, and dried in an oven at 60 °C. Finally, the PANI_Al_2O_3 composite was characterized by FTIR and XRD.

2.5. Polysulfone Sulfonation

A total of 10 g of polysulfone (PSU) was dissolved in 100 mL of chloroform to obtain a 10% (w/v) polysulfone solution. Then, in a three-neck flask, the polysulfone solution was heated to a constant temperature of 40 °C while stirring with a magnetic stirrer. A total of 20 mL of 75% sulfuric acid was gradually added to a three-neck flask, which was purged with nitrogen gas. The synthesis of sulfonated polysulfone (SPSU) was carried out for 60 minutes in an acid chamber. The sulfonated polysulfone was dried for 8 to 10 hours.

2.6. Determination of Sulfonation Degree of PSU and SPSU

Polysulfone and SPSU were weighed at 0.1 g and soaked in 10 mL of 1 N NaOH for 3 days. The remaining NaOH was then titrated with 0.9363 N HCl, and three drops of phenolphthalein indicator were used to determine the endpoint of the titration process. Titration was performed until the color changed from pink to colorless. The degree of sulfonation (SD) was obtained using the following equation:

$$SD = \frac{(V_{blank}\ (mL) - V_{sample}\ (mL)) \times N_{HCl} \times EW_{SO3} \times 100\%}{\text{Sample weight (mg)}} \quad (1)$$

Description:

V_{blank} = Volume of blank HCl (mL)

V_{sample} = Volume of sample HCl (mL)

N = Normality of HCl (N)

EW = equivalent weight (g/ek)

2.7. Synthesis of SPSU-PANI_Al_2O_3 Composite Membranes

A total of 1.0 g of SPSU was dissolved in 10 mL of dimethylacetamide. After homogenization, 1.0 g of PANI_Al_2O_3 (3.0%, 7.5%, 10.0%, and 12.5%) was added, and the reaction temperature was set to 50 °C. The resulting composite was sonicated for 15 minutes at 50 °C, followed by casting onto a glass plate. The resulting membrane was immersed in 1 M H_2SO_4 at 50-60 °C for 15 hours, and washed several times with distilled water. Polysulfone and SPSU were weighed at 0.1 g and soaked in 10 mL of 1 N NaOH for 3 days.

2.8. Determination of Water Uptake Membranes and Composite Membranes (SPSU, SPSU-PANI, SPSU-PANI_Al_2O_3)

The SPSU, SPSU-PANI, and SPSU-PANI_Al_2O_3 membranes were cut into 1 cm × 1 cm pieces and dried in an oven at 100 °C for 2 hours, after which they were weighed to determine their dry weight. After drying, the membranes were immersed in deionized water at room temperature for 24 hours. They were removed and cleaned with tissue, then weighed as wet weight. Weighing was performed to determine the difference in membrane weight between wet and dry conditions.

$$\text{Water uptake} = \frac{\text{wet weight - dry weight}}{\text{dry weight}} \times 100\% \quad (2)$$

2.9. Synthesis of SPSU-PANI_Al_2O_3 Membrane Electrode Assembly (MEA) Using Pt (Anode, A)/Hemin (Cathode, K) Catalyst

Synthesis of MEA from SPSU-PANI_Al_2O_3 composite membranes was conducted by pressing the composite membranes onto electrodes coated with catalysts using a hot press method at a temperature of 130 °C for 2 minutes. The electrode consisted of an anode and a cathode, each coated with a catalyst. The electrode used was carbon paper. The Pt catalyst on the anode (A) was prepared by mixing 5% (w/w) Pt with a 5% (w/w) membrane solution in dichloromethane to form a paste. The paste was then spread on a glass plate and dried. The same method was applied to synthesize a 0.5% hemin catalyst on the cathode (K). The MEA was produced in three and seven layers.

2.10. Determination of Methanol Permeability of MEA SPSU-PANI_Al_2O_3 Using Pt Catalyst (Anode, A)/Hemin (Cathode, K)

Methanol permeability was measured at room temperature using the cell diffusion method. The membrane was placed between two cells/compartments (A and B). Initially, compartment A contained a 1 M methanol solution (CA) as the feed side, and compartment B contained distilled water as the permeation side. Both compartments were stirred using a magnetic stirrer at a constant speed throughout the testing process. Approximately 10 mL of solution was withdrawn from compartment B at 15, 30, 45, and 60 minutes (permeation times), and each sample was weighed to calculate its density. The same procedure was performed for methanol concentrations of 2, 3, 4, and 5 M. Previously, a calibration curve was prepared between the concentration and density of standard methanol solutions with concentrations of 0.5, 1.0, 1.5, and 2.0 M. This calibration curve is used to calculate the methanol concentration in compartment B. The permeability of methanol can be calculated from the slope obtained by interpolating the methanol concentration against the permeation time.

2.11. Determination of Proton Conductivity of MEA SPSU-PANI_Al_2O_3 Using Pt (Anode, A)/Hemin (Cathode, K) Catalyst

The proton conductivity of MEA based composite membrane was determined by measuring impedance using Electrochemical Impedance Spectroscopy (EIS). The

membrane was measured in a two-electrode configuration, in which the material served as the active element connected directly to the measurement system. The testing was conducted by applying a small AC signal under open-circuit conditions with an amplitude of 10 mV. The measurement frequency range was 10 kHz with a logarithmic distribution. The data obtained consisted of complex impedance values, which were then presented in the form of a Nyquist plot to analyze the material's electrical characteristics, particularly its resistance and charge transport mechanisms within the system. Proton conductivity can be measured using the following equation:

$$\sigma = l/RA \quad (4)$$

Description:

σ = proton conductivity

l = distance between electrodes

A = area of the membrane being tested

R = membrane resistance obtained from measurements

2.12. Performance Testing of a Fuel Cell (DMFC) Using a Single Cell

The cell potential, or voltage, in a fuel cell system was measured using two compartments: the anode and cathode systems at 60 ^{o}C. Compartment A, as the anode system, was filled with 100 mL of 1 M methanol solution. Compartment B, as the cathode system, was empty but bubbled with oxygen. The MEA membrane was attached to the center of both vessels. The loading of 5% Pt catalyst used on both the anode and cathode was 2.1 mg/cm^2, while the loading of 0.5% hemin catalyst was approximately 1.2 mg/cm^2, with an MEA active area of 2 × 2 cm^2. Thus, connect each compartment to the positive and negative terminals. The cell potential is measured with a voltmeter, as in a fuel cell (Figure 1).

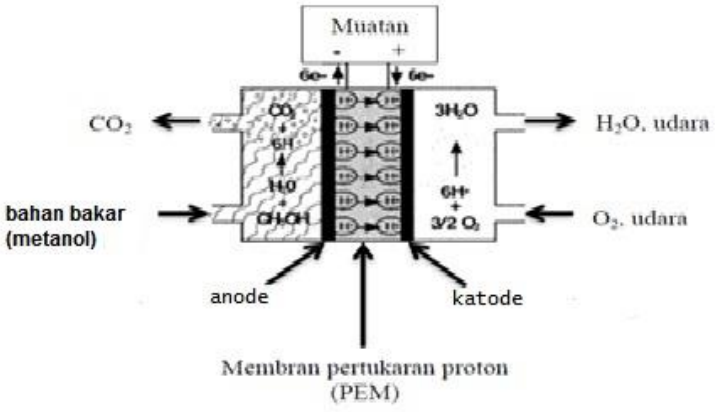

Figure 1. Principles of the DMFC system

2.13. Electrochemical Properties Test of Catalyst

The electrochemical properties of the sample were analyzed using a potentiostat. This cyclic voltammetry (CV) test employed a 3-electrode system consisting of a working electrode (glassy carbon), a reference electrode (Ag/AgCl (3 M NaCl)), and a counter electrode (Pt-coiled). The CV test was conducted at a scan rate of 5 mV s^{-1} in a potential window of 0.0-1.1 V vs. RHE in a 0.5 M H_2SO_4 solution. The cyclic voltammogram was then recorded using specialized software on a computer.

3. Results and Discussion

3.1. Bioactive Compounds *Spondias mombin* Leaf Extract (SMLE)

The green synthesis of Al_2O_3 nanoparticles relies on compounds that have a dual purpose. The first is as reducing agents for the metal ions and as capping agents [16]. The reduction is facilitated by primary functional groups, including carboxyl (-COOH), hydroxyl (-OH), amine (-NH_2), ether (-CO), and carbonyl (-C=O). Alkaloids supply the weak bases required for the synthesis, while saponins cap the growing nanoparticles. This results in well-grained structures. The presence and nature of these constituents were confirmed by the FTIR spectrum (Figure 2), which showed a distinct set of vibrational bands: O–H stretching at 3344 cm^{-1}, C–H (sp^3–s) stretching at 2926 cm^{-1}, C=O streching at 1714 cm^{-1}, O-H bending at 1608 cm^{-1}, N–H bending at 1516 cm^{-1}, C–N bending at 1444 cm^{-1}, C–H bending at 1331 cm^{-1}, C–N aromatic at 1203 cm^{-1}, C–N stretching at 1039 cm^{-1}, and C–H aromatic bending between 868-709 cm^{-1}. The N–H and C–N vibrations detected in the SMLE water fraction confirmed the characteristic presence of alkaloid compounds containing a nitrogen atom within

a cyclic ring.

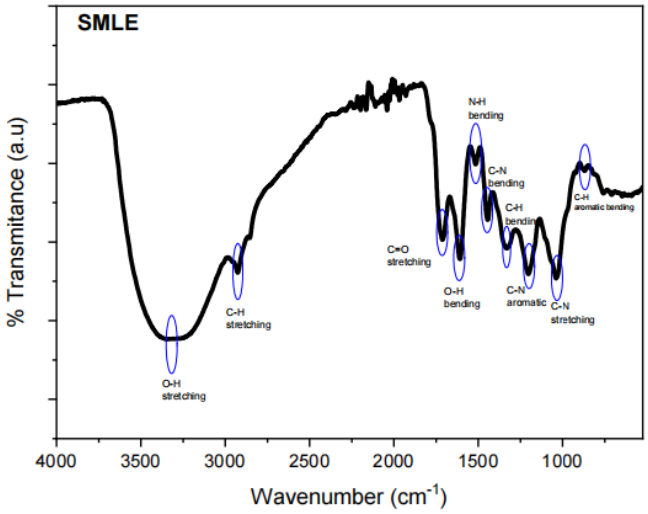

Figure 2. FTIR spectrum of s*pondias mombin* leaf extract

3.2. Al_2O_3 nanoparticles and Sulfonated Polysulfone-Polyaniline_Al_2O_3 Composite Membranes (SPSU-PANI_Al_2O_3)

Al_2O_3 nanoparticles (Al_2O_3.NP) produced in medium *Spondias mombin* leaf extract were identified by their particle size of 33 nm. Nanoparticles offer a significantly large surface area, which is expected to enhance their functionality, including as composite support materials and catalyst supports. The Al_2O_3 nanoparticles obtained showed excellent structural stability, as demonstrated by a zeta potential value of -28.8 mV (Figure 3a). A zeta potential value is considered good if it is in the range of ± 31-60 mV. According to Lowry et al. [17], since there is more electrostatic repulsion between particles, a higher zeta potential value shows improved overall particle stability. On the other hand, nanomaterial aggregation is indicated by a low zeta potential value [18]. The stability of Al_2O_3.NP is influenced by the presence of the saponin biocapping agent in the SMLE [19]. The stability of these nanoparticles has a linear effect on their thermal stability, as evidenced by the low weight loss of 0.774% due to the evaporation of water and organic molecules at temperatures ranging from 104.45 to 373.35 °C, without degradation of the structure (Figure 3b).

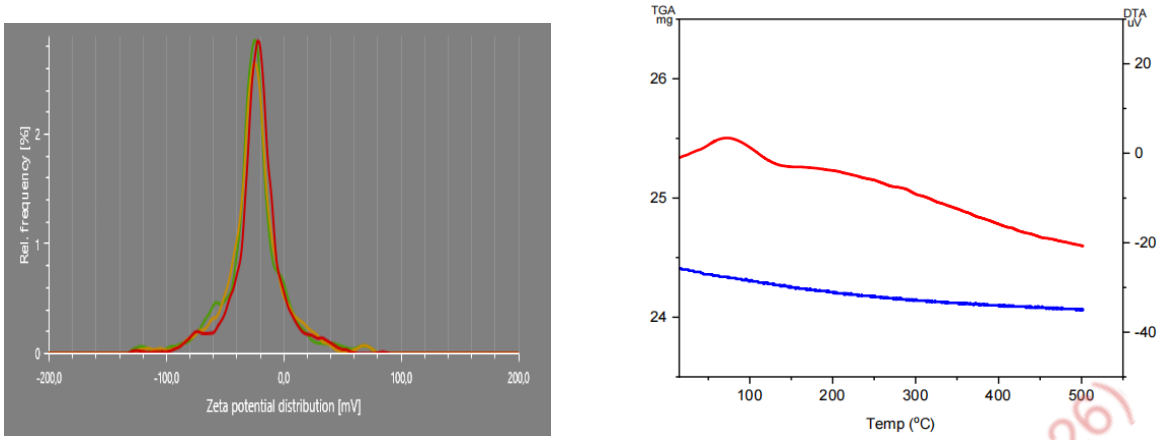

(a) (b)

Figure 3. (a) Zeta potential, and (b) termogram TGA/DTA Al_2O_3.NP

The morphological properties of Al_2O_3.NP were studied using SEM (Figure 4a). The development of nanoparticles was stabilized by the biocapping agent saponins found in SMLE [19]. Based on Figure 4(b), the elemental distribution pictures of Al_2O_3 demonstrate exceptional purity, with 55.9.0% Al and 44.1% O forming the material. The SAED pattern reveals that the sample exhibits diffuse rings, indicative of an amorphous structure, as well as three distinct, fine ring patterns, indicating the presence of crystalline particles. According to SAED (Figure 4c) and database analyses, the sample contains ring patterns, indicating the alumina has a crystalline structure. The bright field (BF) TEM image (Figure 4d) shows the irregular morphology of the alumina nanoparticles. In good agreement with the SAED patterns, the HRTEM image (Figure 4e-4f) shows that the alumina nanoparticles are composed of particles with amorphous and crystalline structures (with lattice fringes). A combination of STEM and EDX analysis (Figure 4g-4h) reveals that the sample contains oxygen and aluminum elements, indicating an alumina composition. Electron energy loss spectra reveal that the alumina has a gamma alumina structure, as presented in the EELS database [20]. Alumina, particularly in its gamma phase, possesses a range of industrial applications and can be extensively utilized.

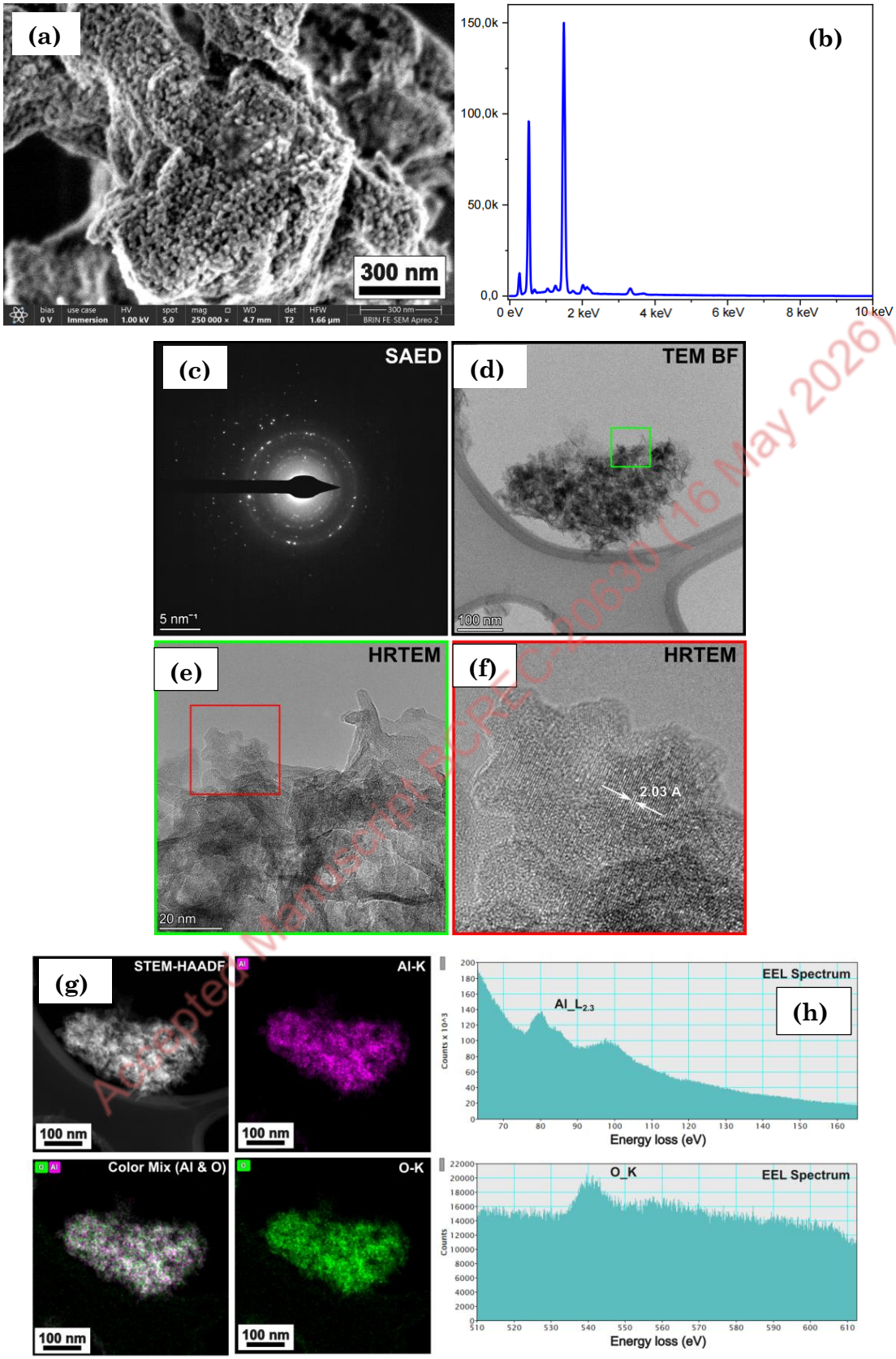

Figure 4. (a) SEM images, (b) elemental mapping, (c) SAED, (d) TEM, (e-f) HRTEM, (g) STEM and (h) EEL of Al_2O_3

The presence of Al_2O_3 nanoparticles in the SPSU-PANI composite membrane, as indicated by FTIR and XRD analysis, affects the performance of the composite membrane in its application as a component in fuel cells. Figure 5 shows the FTIR spectra of Al_2O_3, PANI_Al_2O_3, and SPSU-PANI_Al_2O_3. The detection of the O confirmed the SMILE–H stretching vibration at 3307 cm^{-1} and the Al-O stretching vibration at 560 cm^{-1} in the Al_2O_3 FTIR spectrum. At 800-500 cm^{-1}, the Al-O stretching vibration is visible. 715.6 cm^{-1} of Al-O stretching vibration was found in AlO_4^- [21]. PANI_Al_2O_3 and SPSU-PANI_Al_2O_3 FTIR spectra were acquired. As evidence of PANI's existence, N-H stretching aromatic, C=C stretching in quinoide and benzenoide rings, and C-N stretching vibrations were found at 2314, 1587, and 1328 cm^{-1}, respectively. Specific spectra at 588, 1177, 1259, and 2979 cm^{-1}, which show C-S stretching, symmetrical C-SO_2-C stretching, C-O-C stretching, and S=O stretching vibrations, respectively, are indicative of the distinctive polysulfone spectra. The shift of the Al-O stretching vibration at 881 cm^{-1} indicated that Al_2O_3.NP had been successfully integrated into the composite membrane.

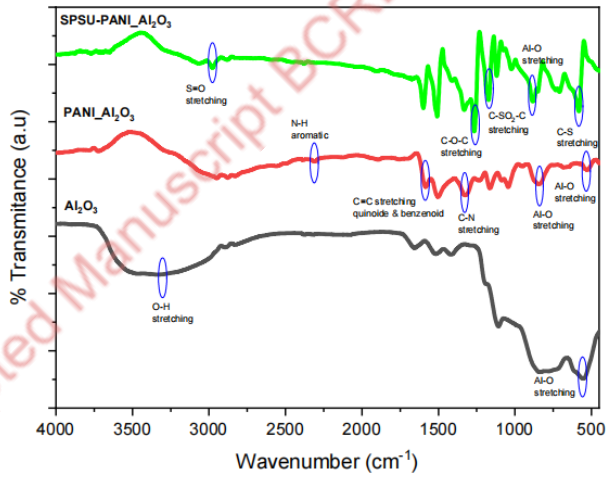

Figure 5. FTIR spectra of Al_2O_3, PANI_Al_2O_3, and SPSU-PANI_Al_2O_3

As shown in Figure 6, XRD measurements were performed to analyze the structure of the samples. In light of the analysis's findings in relation to the JCPDS-ICDD No. 46-1212 literature data, distinct peaks were found with diffraction angles of 2θ, namely 16.28°; 25.47°; 26.01°; 30.81°; 32.96°; 35.06°; 38.70°; 39.05°; 42.36°; 49.57°; 54.60°; 57.64°; 60.44°; 64.41°; 66.74°; 70.57°; and 74.36°, indicating the existence of a crystalline phase. These analysis results are consistent with the

HRTEM test results, which also show the presence of an amorphous phase and the crystallinity of Al_2O_3.NP produced by green synthesis using SMLE, leading to the presence of a crystalline phase in the SPSU-PANI composite membrane, which has an amorphous phase with broad, weak diffraction peaks from PANI at angles of 2θ of 14.86°; 29.05°; and 34.94° (COD-90006293), forming angles of 2θ of 17°; 25°. The existence of a crystalline phase in polymers can reduce ion conductivity [22]. Under these conditions, the crystalline region, characterized by ordered polymer chains, can limit or inhibit ion mobility through the material.

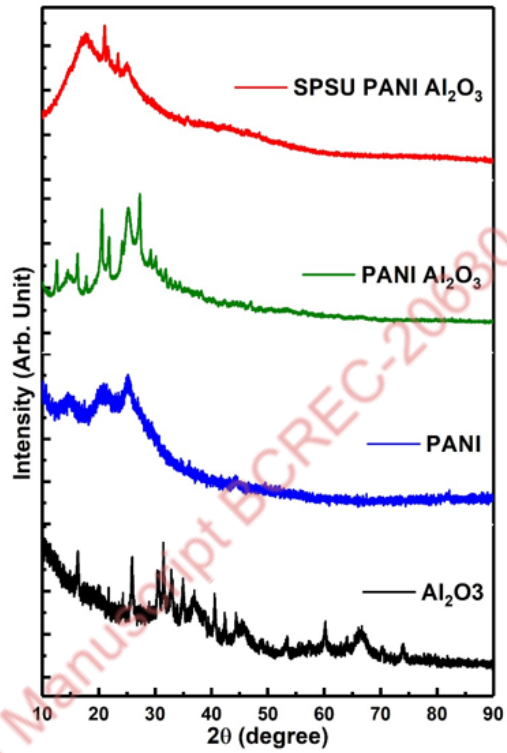

Figure 6. XRD pattern of Al_2O_3, PANI, PANI_Al_2O_3, and SPSU-PANI_Al_2O_3

In contrast, the water uptake value required for fuel cell applications can be increased by the inclusion of Al_2O_3 NP (Figure 7). The capacity of a membrane to hold or absorb water is known as water uptake. Water molecules are necessary as carriers for proton conduction in the PEM [22], since water molecules aid in proton transport and dissociation [23]. This suggests that an increase in water uptake in sulfonated polymer composite membranes will cause a higher solute concentration, which is necessary to enhance proton conductivity. However, a high water content can cause the membrane to become less mechanically stable [24].

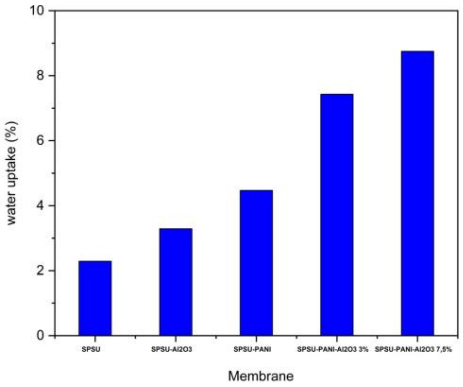

Figure 7. Water uptake value of SPSU, SPSU-Al_2O_3, SPSU-PANI, and SPSU-PANI_Al_2O_3

3.3. Membrane Electrode Assembly based on Sulfonated Polysulfone-Polyaniline_Alumina (SPSU-PANI_Al_2O_3) Composite for Fuel Cell Technologies

The membrane electrode assembly (MEA) based on sulfonated polysulfone-polyaniline-alumina (SPSU-PANI_Al_2O_3) composite using platinum catalyst on the anode, Pt 5% (A), and hemin on the cathode, hemin 0,5% (K), applied to a direct methanol fuel cell (DMFC). Methanol permeability, proton conductivity, power density, and the catalyst's electrochemical characteristics all demonstrate the fuel cell's performance.

In a DMFC system, methanol diffuses from the anode to the cathode through the MEA. This membrane serves as a transport medium for hydrogen ions (H^+) generated by the oxidation reaction at the anode and as a separator between the two electrodes. According to [25], the reactions occurring in a DMFC are as follows:

Anode : $CH_3OH_{(l)} + H_2O_{(l)} \rightarrow CO_{2(g)} + 6H^+ + 6e^-$

Cathode : $\underline{^3/_2O_{2(g)} + 6H^+ + 6e^- \rightarrow 3H_2O_{(l)}}$

Overall reaction : $CH_3OH_{(l)} + {}^3/_2O_2 \rightarrow CO_{2(g)} + 2\underline{H_2O_{(l)}}$

Increasing the membrane thickness can reduce methanol permeability [26], Conversely, an increase in membrane thickness (the distance electrons must travel) will increase ohmic resistance. In other words, ohmic resistance is proportional to membrane thickness. Meanwhile, methanol diffusion through the membrane or high ohmic resistance can reduce the performance of the direct methanol fuel cell (DMFC), as evidenced by a decrease in cell potential. In this study, the MEA based on SPSU-

PANI_Al_2O_3, an increase in membrane thickness to 3 and 7 layers, respectively, with membrane thickness ranges of 343–424 and 575–791 µm (Figure 8a), resulted in methanol permeability that was not significantly different (p-*value* (0,14) > α (0,05) (Figure 8b). An increase in thickness did not significantly increase methanol permeability. This was confirmed by an ANOVA statistical analysis of the effect of membrane thickness on methanol permeability, conducted at a significance level (α) of 0.05, which showed that the p-value (0.14) was greater than α (0.05). The reason why an increase in membrane thickness does not reduce methanol permeability is the structural and morphological effects resulting from it's not optimal hot pressing during the MEA fabrication process, which leads to reduced contact between the catalyst layer and the membrane (PEM) [27]. Based on the results of the morphological analysis of the MEA cross-section (Figure 9), it was found that as the membrane thickness increases or the number of layers in the membrane increases, the number of interlayer gaps in a single MEA assembly also increases; consequently, an increase in membrane thickness is not accompanied by an improvement in the membrane's barrier properties against methanol diffusion. Therefore, to reduce the ohmic resistance, the study utilized an MEA with three layers.

The membrane electrode assembly consists of a gas diffusion layer (GDL) made of carbon paper, a catalyst layer (CL) on the anode and cathode sides, and a proton exchange membrane (PEM) in between. Within the CL, the ionomer (polymer) plays a key role in proton transport between the CL and the PEM, and helps the reactant (methanol) diffuse to the catalyst surface [28]. the catalyst is not directly control membrane diffusion characteristics. However, based on an ANOVA statistical analysis of the effect of the catalyst on methanol permeability in the MEA, the p-value (0.95) was greater than α (0.05). This ensures that the permeability of methanol in the MEA is not affected by the catalyst.

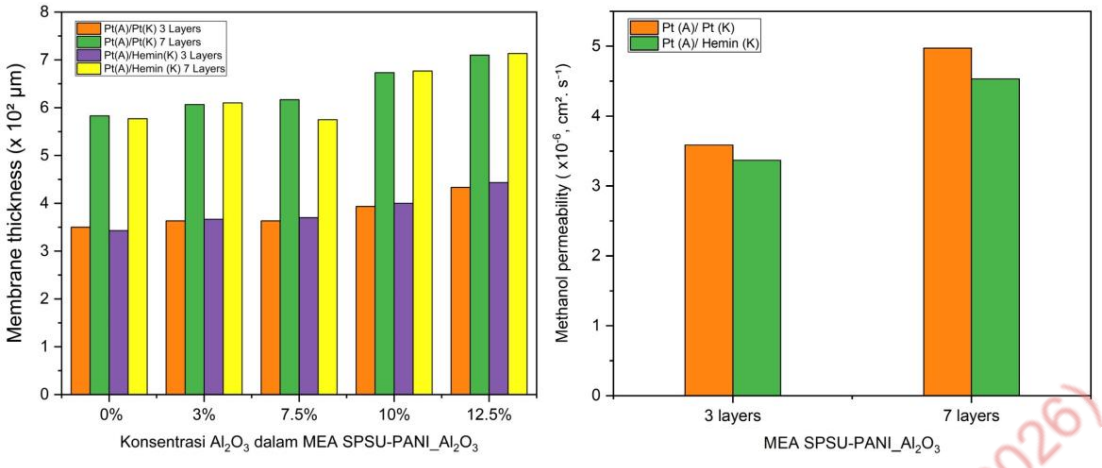

(a) (b)

Figure 8. (a) Membrane thickness, and (b) methanol permeability of MEA SPSU-PANI_Al_2O_3 using Pt 5% (A)/Pt 5% (K) and Pt 5% (A)/Hemin 0.5% (K) catalysts in three and seven layers

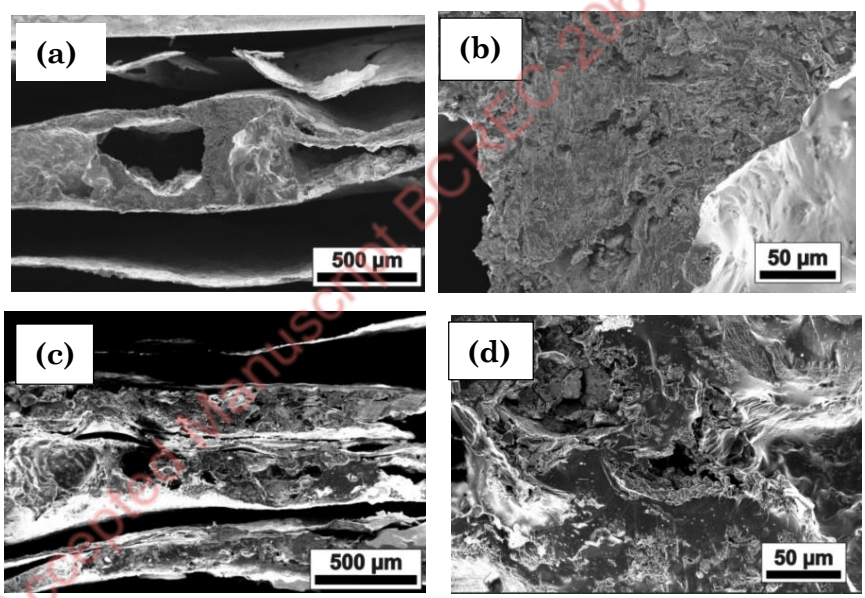

Figure 9. Cross-sectional morphology of MEA SPSU-PANI_Al_2O_3 in (a-b) three, and (c-d) seven layers using Pt (A)/Hemin (K) catalyst

Meanwhile, based on the TGA/DTA analysis (Figure 10), the SPSU-PANI_Al_2O_3-based MEA exhibited a mass loss of 1.0–1.5%. A mass loss of less than 5% can be considered insignificant [28], so the SPSU-PANI_SiO_2/Al_2O_3-based MEA (20) is classified as having good thermal stability. The composite material in the SPSU-based membrane is capable of shifting the first thermal degradation temperature to a higher value. The first thermal degradation temperature recorded for the SPSU

membrane is 200 °C, whereas SPSU-PANI_Al_2O_3-based MEAs using Pt (A)/hemin (K) and Pt (A)/Pt (K) catalysts were indicated at 240 and 225 °C, respectively. Thus, it can be concluded that all MEA SPSU-PANI_SiO_2/Al_2O_3 remain thermally stable at 200–250 °C, a temperature high enough for DMFC operation.

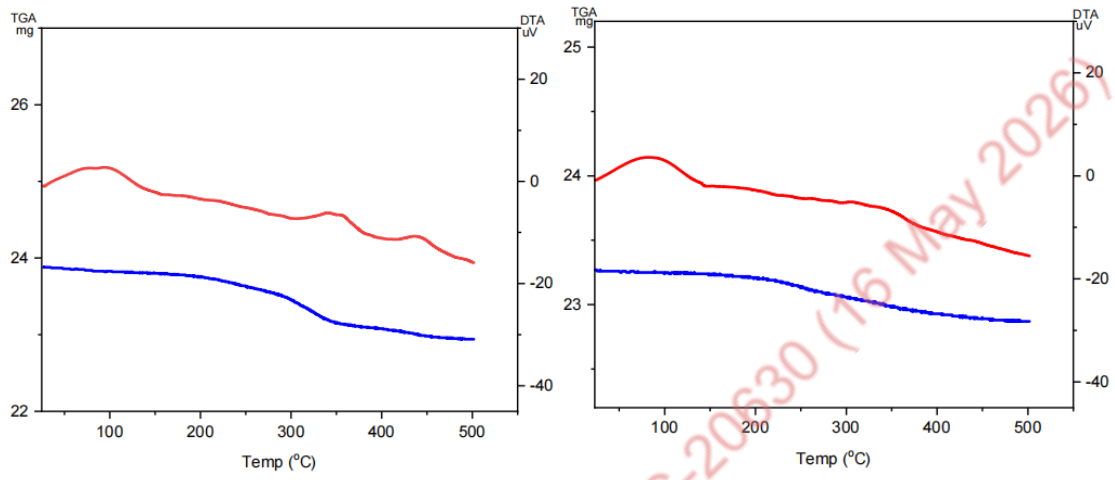

(a) (b)

Figure 10. TGA/DTA thermograms of MEA SPSU-PANI_Al_2O_3 with (a) hemin and (b) Pt catalysts on the cathode

The performance of direct methanol fuel cells (DMFC) can be influenced by various factors such as temperature, catalysts, and the membrane electrode assembly (MEA) fabrication process [29]. Meanwhile, methanol diffusion is highly dependent on temperature and the concentration of methanol at the anode [30]. Therefore, the polarization behavior of the SPSU-PANI_SiO_2/Al_2O_3-based MEA in this study was observed in a single-cell DMFC at 60 °C in 1 M methanol. Performance is tested specifically in the activation and ohmic regions of the polarization curve. In the activation region, a decrease in voltage occurs due to the presence of excess activation potential resulting from the slow redox reaction at the anode and particularly at the cathode because the ORR kinetics are much slower than those of the HOR, as well as the diffusion of methanol (methanol crossover). Therefore, the activation energy loss depends on the catalyst activity. The better the catalyst used, the lower the activation energy required. In addition, a voltage drop also occurs in the ohmic region due to the resistance encountered by electrons flowing through the MEA layers, resulting in

ohmic losses arising from (i) the total resistance of the components (constituent materials), (ii) the interfacial contact resistance between components, and (iii) the resistance to proton transport.

The measured initial voltage can be used as an indicator of the membrane's ability to suppress methanol. The initial voltage (Open Circuit Voltage, OCV) is the voltage across the cell before it is loaded; it is related to fuel crossover, the phenomenon of electrons passing through the membrane, as well as internal current. The OCV values for the Pt (A)/Pt (K) and Pt (A)/hemin (K) catalysts were obtained using an MEA based on a 12.5% SPSU-PANI_Al_2O_3 composite membrane; and SPSU-PANI_Al_2O_3 3% composite membranes, respectively, were 0.993 V and 0.925 V (Figures 11a–b). These voltage values are higher for the SPSU-PANI_Al_2O_3 composite membrane than for the SPSU-PANI, SPSU-Al_2O_3, and SPSU membranes, in that order: 0.781 V; 0.759 V; 0.740 V; and 0.714 V (Figure 11c).

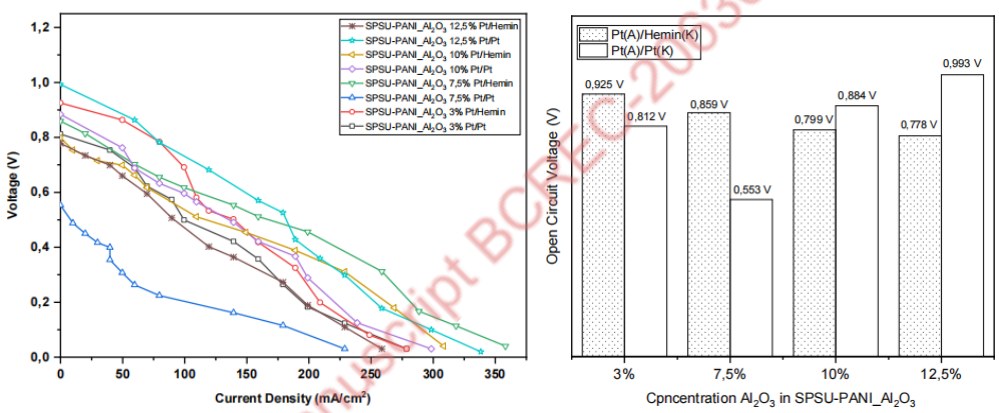

(a) (b)

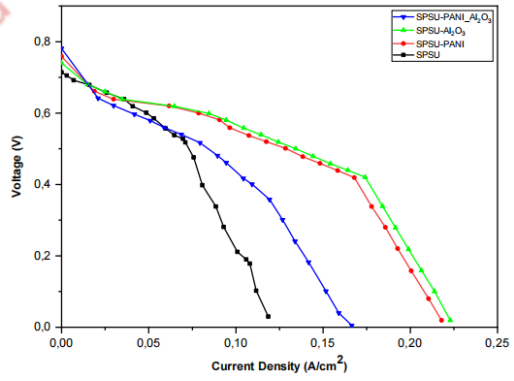

(c)

Figure 11 OCV values in the DMFC system on (a–b) MEA and (c) composite membrane based on sulfonated polysulfone

The effect of the catalyst on the performance of the direct methanol fuel cell (DMFC) is also evident in the power density achieved, where SPSU-PANI_Al_2O_3 12.5% with Pt (A)/Pt (K) > SPSU-PANI_Al_2O_3 7.5% with Pt (A)/hemin (K) catalyst, at 94.23 mW/cm² and 90.76 mW/cm², respectively (Figure 12a). These power density values are higher for the SPSU-Al_2O_3 7.5% composite membrane than for SPSU-PANI > SPSU-PANI-Al_2O_3 7.5% > SPSU, in that order: 73.15 mW/cm²; 70.35 mW/cm²; 43.82 mW/cm²; 36.78 mW/cm² (Figure 12b). There are several factors that can affect both the membrane power density and the current density, namely: (i) The proton transport mechanism in the sulfonate-based membrane leads to greater adsorption and retention of water molecules; (ii) The hydrophilicity of inorganic nanocomposite materials in the membrane that affects proton transport; and (iii) The proton conductivity of the composite membrane [31].

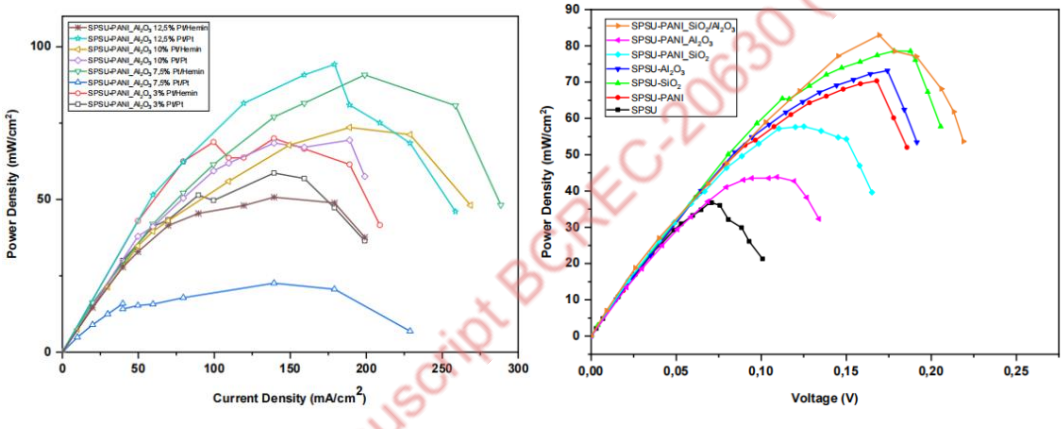

(a) (b)

Figure 12 Power density of (a) MEA and (b) composite membrane based on sulfonated polysulfone (SPSU)

The performance of the DMFC is confirmed by the current density limit, which is the maximum electrical current per unit cross-sectional area that can flow through the membrane without causing damage to the DMFC system. The lowest current density limit values for each MEA were obtained as follows: SPSU-PANI_Al_2O_3 7.5% using either the Pt (A)/hemin (K) or Pt (A)/Pt (K) catalysts, with values of 126 mA/cm² and and 100 mA/cm² (Figure 13a-b). The current density limit of this MEA is lower than that of the composite membrane, where the current density limit of the SPSU-PANI_Al_2O_2 composite membrane is 150 mA/cm² (Figure 13c). The low current density limit indicates high methanol resistance due to cross-linking between the

composite material and the polymer, which can reduce the size of the hydrophilic channels, thereby increasing the bending of the methanol/H_2O diffusion path and reducing the methanol flux [32].

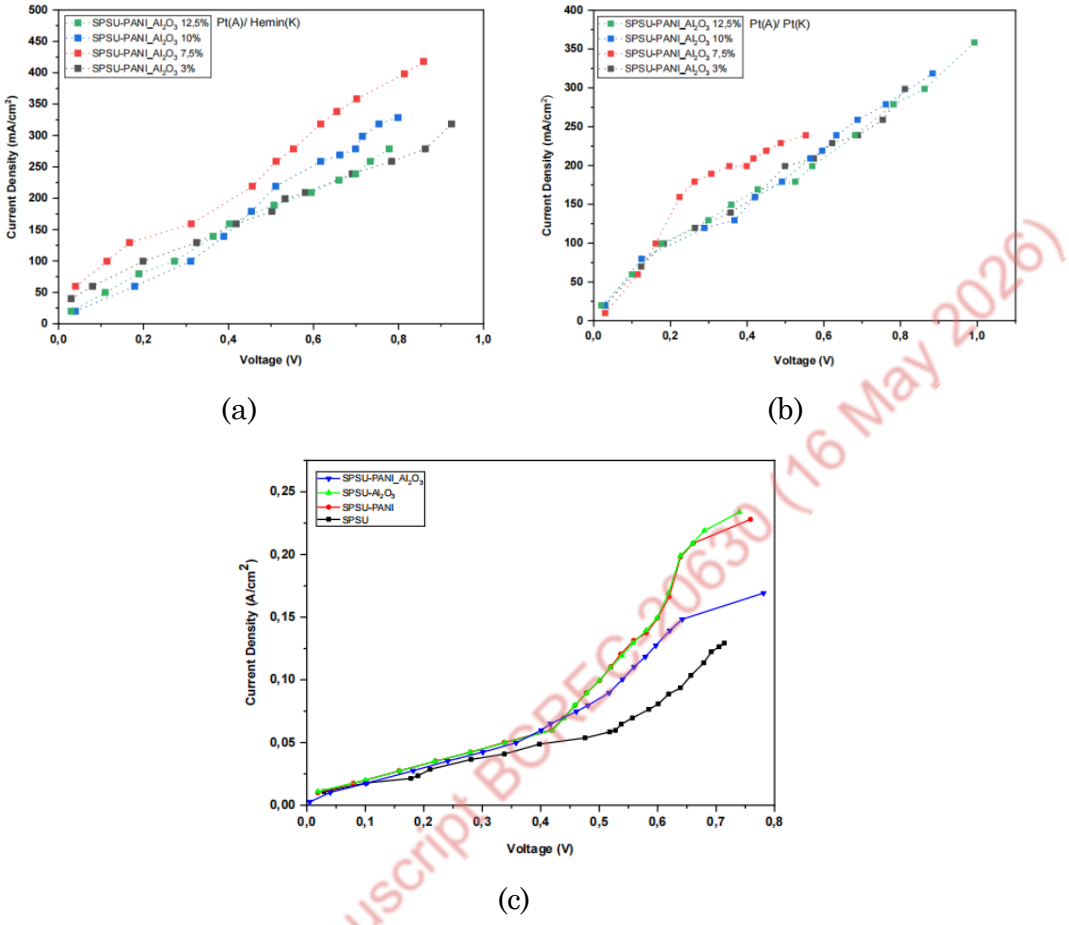

Figure 13 Current density limits for single-cell DMFCs (a) MEA and (b) composite membrane based on sulfonated polysulfone (SPSU)

The mechanism of proton conduction is mediated by hydrogen bonds between protonated species and their surroundings. The MEA based on SPSU-PANI_Al_2O_3 7.5% using a Pt catalyst at the cathode yields a higher proton conductivity than other MEAs, specifically 9.95×10^{-4} S/cm (Tabel 1) based on oxidative stability, as indicated by the lowest weight loss and the maximum number of ions that can be exchanged in a membrane structure, as indicated by the ion exchange capacity (IEC) value, even though this value is two to three orders of magnitude lower than Nafion and significantly lower than many reported hydrocarbon PEM systems. This is influenced by the interfaces between the layers within the MEA, on both the anode and cathode sides, namely the proton exchange membrane/catalyst layer (PEM/CL) interface, the catalyst layer/microporous layer (CL/MPL) interface, and the microporous

layer/carbon fiber paper (MPL/CFP) interface. These interfaces in the MEA play a crucial role in the performance and durability of fuel cells, particularly in relation to mechanical adhesion, mass transport, charge transfer, and heat conduction [33]. Based on the results of cyclic voltammetry tests on the electrochemical cells, the catalysts exhibited relatively similar reduction peaks when using either the Pt (A)/hemin (K) or Pt (A)/Pt (K) catalysts via the 2-electron pathway at the cathode (Figure 13), with the following reaction:

$$O_{2(g)} + 2H^{+}_{(aq)} + 2e^{-} \longrightarrow 2H_2O_{2(aq)} \quad E = 0{,}48\text{-}0{,}52\ V$$

$$H_2O_{2(aq)} + 2H^{+}_{(aq)} + 2e^{-} \longrightarrow 2H_2O_{(l)} \quad E = 1{,}22\ V$$

Table 1 Proton conductivity of MEA based on sulfonated polysulfone composite

MEA	*Water Uptake* (%)	IEC (meq/g)	Oxidative Stability (%)	membrane thickness (µm)		Proton Conductivity (S/cm)	
				Pt 5% (A)/Pt 5% (K)	Pt 5% (A)/ 0,5% hemin (K)	Pt 5% (A)/Pt 5% (K)	Pt 5% (A)/ 0,5% hemin (K)
SPSU-PANI	3,25	0,601	94,38	350	343	$5{,}89 \times 10^{-6}$	$3{,}79 \times 10^{-6}$
SPSU-PANI_Al_2O_3 3%	7.43	0.667	92.69	353	351	$9{,}72 \times 10^{-4}$	$4{,}86 \times 10^{-4}$
SPSU-PANI_Al_2O_3 7,5%	8.75	0.749	97.28	364	376	$9{,}95 \times 10^{-4}$	$2{,}22 \times 10^{-4}$
SPSU-PANI_Al_2O_3 10%	6.45	0.681	94.73	394	406	$9{,}33 \times 10^{-4}$	$2{,}89 \times 10^{-4}$

SPSU-PANI_Al_2O_3 12,5%	5,.45	0.540	96.84	424	424	8,79 x 10^{-4}	4,05 x 10^{-4}

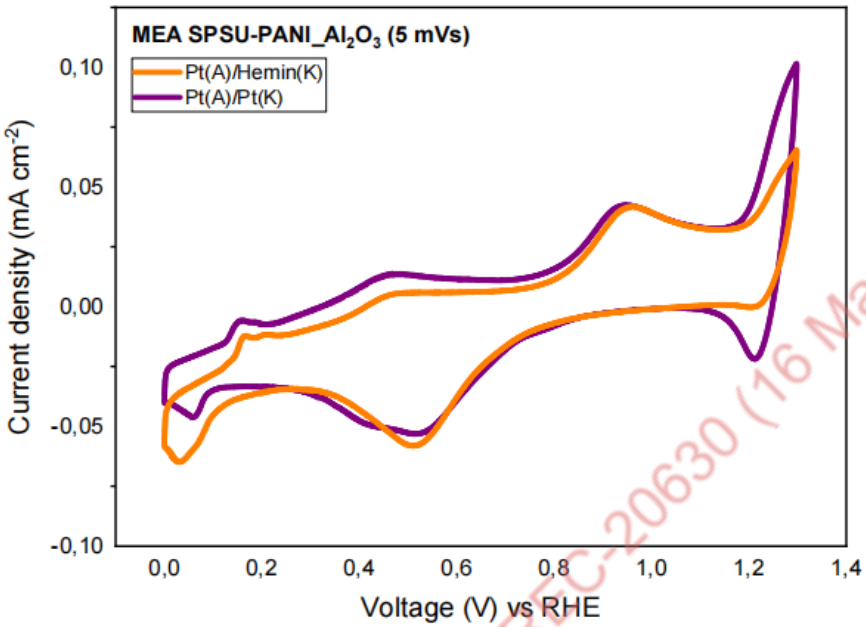

Figure 13. Cyclic voltammetry curve of MEA based on SPSU-PANI_Al_2O_3 Composite

4. Conclusions

Alumina Nanoparticles in a medium of *Spondias mombin* leaf extract of A sulfonated polysulfone-polyaniline_alumina Membrane Electrode Assembly and a hemin catalyst at the cathode was successfully incorporated and characterized. The alumina nanoparticles synthesized in a medium *Spondias mombin* leaf extract exhibit a particle size of 33 nm. The MEA based on sulfonated polysulfone-polyaniline_alumina 7.5% composite with the hemin catalyst on the cathode in a fuel cell (DMFC) demonstrated good structural and thermal stability, low methanol crossover and high power density 90.76 mW/cm^2, but low proton conductivity. The hemin catalyst produces reduction peaks at cell potentials 0.48-0.52 V dan 1,22 V that are relatively similar to those of the Pt catalyst in the oxygen reduction reaction during the electrochemical cell test. Therefore, the hemin catalyst at the cathode has demonstrated potential as an alternative to the Pt catalyst for fuel cell technologies.

5. Acknowledgment

We would like to express our gratitude to the Ministry of Education, Culture, Research, and Technology of Indonesia through Grant Research Number SKU-137/UN2.R3/HKP.05/2022; ILRC UI. IPB University's Laboratory of Physical Chemistry; Chemistry Laboratory of the Faculty of Mathematics and Natural Sciences, University of Indonesia; Physics Engineering Laboratory of the Bandung Institute of Technology; and the National Research and Innovation Agency (BRIN) for helping to establish this research.

6. References

[1] Sigwadi, R., Mokrani, T., Dhlamini, M.S., Nonjola, P., Msomi, P.F. (2019). Nafion®/ sulfated zirconia oxide-nanocomposite membrane: the effects of ammonia sulfate on fuel permeability. *Journal of Polymer Research*, 26(5) DOI: 10.1007/s10965-019-1760-2.

[2] Baker, A.M., Wang, L., Johnson, W.B., Prasad, A.K., Advani, S.G. (2014). Nafion membranes reinforced with ceria-coated multiwall carbon nanotubes for improved mechanical and chemical durability in polymer electrolyte membrane fuel cells. *Journal of Physical Chemistry C*, 118(46), 26796–26802. DOI: 10.1021/jp5078399.

[3] Lufrano, F., Baglio, V., Di Blasi, O., Staiti, P., Antonucci, V., Aricò, A.S. (2012). Solid polymer electrolyte based on sulfonated polysulfone membranes and acidic silica for direct methanol fuel cells. *Solid State Ionics*, 216, 90–94. DOI: 10.1016/j.ssi.2012.03.015.

[4] Padmavathi, R., Karthikumar, R., Sangeetha, D. (2012). Multilayered sulphonated polysulfone/silica composite membranes for fuel cell applications. *Electrochimica Acta*, 71, 283–293. DOI: 10.1016/j.electacta.2012.04.015.

[5] Maharana, T., Sutar, A.K., Nath, N., Routaray, A., Negi, Y.S., Mohanty, B. (2014). Polyetheretherketone (PEEK) Membrane for Fuel Cell Applications. In: *Advanced Energy Materials*. Wiley, pp. 433–464.DOI: 10.1002/9781118904923.ch11.

[6] Mulijani, S., Dahlan, K., Wulanawati, A. (2014). Sulfonated Polystyrene Copolymer: Synthesis, Characterization and Its Application of Membrane for Direct Methanol Fuel Cell (DMFC). *International Journal of Materials,*

Mechanics and Manufacturing, 2(1), 36–40. DOI: 10.7763/ijmmm.2014.v2.95.

[7] Nagarale, R.K., Gohil, G.S., Shahi, V.K., Rangarajan, R. (2005). Preparation and electrochemical characterization of sulfonated polysulfone cation-exchange membranes: Effects of the solvents on the degree of sulfonation. *Journal of Applied Polymer Science*, 96(6), 2344–2351. DOI: 10.1002/app.21630.

[8] Rehman, M., Zhang, W., Su, H., Zhang, J., Rhimi, B., Liu, H., Xing, L., Yan, X., Xu, Q. (2024). Review article A review of additional modifications of additives through hydrophilic functional groups for the application of proton exchange membranes in fuel cells. *Journal of Power Sources*, 622(September), 235353. DOI: 10.1016/j.jpowsour.2024.235353.

[9] Njoku, P.C., Akumefula, M.I. (2007). Phytochemical and Nutrient Evaluation of Spondias Mombin Leaves. *Pakistan Journal of Nutrition*, 6(6), 613–615. DOI: 10.3923/pjn.2007.613.615.

[10] Maria Mahimai, B., Kulasekaran, P., Deivanayagam, P. (2021). Novel polysulfone/sulfonated polyaniline/niobium pentoxide polymer blend nanocomposite membranes for fuel cell applications. *Journal of Applied Polymer Science*, 138(41) DOI: 10.1002/app.51207.

[11] Penteado, M.H., Cruz-Cruz, I., Hümmelgen, I.A. (2019). Giant Seebeck coefficient in thin sulfonated polyaniline film based devices. *Organic Electronics*, 67, 153–158. DOI: 10.1016/j.orgel.2019.01.007.

[12] Goudarzi, M., Ghanbari, D. (2015). Synthesis and Characterization of Al(OH)3, Al2O3 Nanoparticles and Polymeric Nanocomposites. J Clust Sci. https://doi.org/10.1007/s10876-015-0895-5

[13] Alhoshan, M., Alam, J., Dass, L.A., Al-Homaidi, N. (2013). Fabrication of Polysulfone/ZnO Membrane: Influence of ZnO Nanoparticles on Membrane Characteristics. *Advances in Polymer Technology*, 32(4) DOI: 10.1002/adv.21369.

[14] Proietti, E., Jaouen, F., Lefèvre, M., Larouche, N., Tian, J., Herranz, J., Dodelet, J.-P. (2011). Iron-based cathode catalyst with enhanced power density in polymer electrolyte membrane fuel cells. *Nature Communications*, 2(1), 416. DOI: 10.1038/ncomms1427.

[15] Maruyama, J., Abe, I. (2007). Fuel Cell Cathode Catalyst with Heme-Like Structure Formed from Nitrogen of Glycine and Iron. *Journal of The*

Electrochemical Society, 154(3), B297. DOI: 10.1149/1.2409865.

[16] Villagran, Z., Anaya-esparza, L.M., Arnulfo, C., Rodr, E., Mart, F. (2024). Plant-Based Extracts as Reducing , Capping , and Stabilizing Agents for the Green Synthesis of Inorganic Nanoparticles. *MDPI*, 13(70), 1–24. DOI: 10.3390/resources13060070.

[17] Lowry, G. V., Hill, R.J., Harper, S., Rawle, A.F., Hendren, C.O., Klaessig, F., Nobbmann, U., Sayre, P., Rumble, J. (2016). Guidance to improve the scientific value of zeta-potential measurements in nanoEHS. *Environmental Science: Nano*, 3(5), 953–965. DOI: 10.1039/c6en00136j.

[18] Wang, H., Liu, Y., Li, M., Huang, H., Shen, H. (2009). Multifunctional TiO2 nanowires-modified nanoparticles bilayer film for all-titanium spiral-shaped dye-sensitized solar cells. *Chemical Communications*, 4(8), 1166–1169.

[19] Kane, S.N., Mishra, A., Dutta, A.K. (2016). Preface: International Conference on Recent Trends in Physics (ICRTP 2016). *Journal of Physics: Conference Series*, 755(1), 8–13. DOI: 10.1088/1742-6596/755/1/011001.

[20] Feret, F.R., Roy, D., Boulanger, C. (2000). Determination of alpha and beta alumina in ceramic alumina by X-ray diffraction. *Spectrochimica Acta Part B: Atomic Spectroscopy*, 55(7), 1051–1061. DOI: 10.1016/S0584-8547(00)00225-1.

[21] Shen, L., Hu, C., Sakka, Y., Huang, Q. (2012). Study of phase transformation behaviour of alumina through precipitation method. *Journal of Physics D: Applied Physics*, 45(21), 215302. DOI: 10.1088/0022-3727/45/21/215302.

[22] Wang, G., Kang, J., Yang, S., Lu, M., Wei, H. (2023). Influence of structure construction on water uptake , swelling , and oxidation stability of proton exchange membranes. *International Journal of Hydrogen Energy*, 50, 279–311. DOI: 10.1016/j.ijhydene.2023.08.129.

[23] Xing, P., Robertson, G.P., Guiver, M.D., Mikhailenko, S.D., Wang, K., Kaliaguine, S. (2004). Synthesis and characterization of sulfonated poly(ether ether ketone) for proton exchange membranes. *Journal of Membrane Science*, 229(1–2), 95–106. DOI: 10.1016/j.memsci.2003.09.019.

[24] Deivanayagam, P., Ramanujam Ramamoorthy, A., Jaisankar, S.N. (2013). Synthesis and characterization of sulfonated poly (arylene ether sulfone)/silicotungstic acid composite membranes for fuel cells. *Polymer Journal*, 45(2), 166–172. DOI: 10.1038/pj.2012.102.

[25] Mallick, R.K., Thombre, S.B., Shrivastava, N.K. (2016). Vapor feed direct methanol fuel cells (DMFCs): A review. *Renewable and Sustainable Energy Reviews*, 56, 51–74. DOI: 10.1016/j.rser.2015.11.039.

[26] Ahmed, M., Dincer, I. (2011). Methanol crossover in direct methanol fuel cells : challenges and achievements. *International Journal of Energy Research*, (July), 1213–1228. DOI: 10.1002/er.

[27] Bayrakceken, A., Erkan, S., Turker, L., Eroglu, I. (2008). Effects of membrane electrode assembly components on proton exchange membrane fuel cell performance. *Journal of Hydrogen Energy*, 33, 165–170. DOI: 10.1016/j.ijhydene.2007.08.021.

[28] Chen, M., Zhao, C., Sun, F., Fan, J., Li, H., Wang, H. (2020). Research progress of catalyst layer and interlayer interface structures in membrane electrode assembly (MEA) for proton exchange membrane fuel cell (PEMFC) system. *eTransportation*, 5, 100075. DOI: 10.1016/j.etran.2020.100075.

[29] Li, J., Wu, H., Cao, L., He, X., Shi, B., Li, Y., Xu, M. (2019). Enhanced Proton Conductivity of Sulfonated Polysulfone Membranes under Low Humidity via the Incorporation of Multifunctional Graphene Oxide. *ACS Applied Nano Materials*, 2, 4734–4743. DOI: 10.1021/acsanm.9b00446.

[30] Baronia, R., Goel, J., Kaswan, J., Shukla, A., Singhal, S.K., Singh, S.P. (2018). PtCo / rGO nano - anode catalyst : enhanced power density with reduced methanol crossover in direct methanol fuel cell. *Materials for Renewable and Sustainable Energy*, 7(27), 1–13. DOI: 10.1007/s40243-018-0134-8.

[31] Gandhimathi, S., Krishnan, H. (2019). Development of proton-exchange polymer nanocomposite membranes for fuel cell applications. *Polymers and Polymer Composites*, 1–10. DOI: 10.1177/0967391119888319.

[32] Lufrano, C., Simari, C., Vecchio, C.L., Arico, A.S., Baglio, V., Nicotera, I. (2020). Barrier properties of sulfonated polysulfone / layered double hydroxides nanocomposite membrane for direct methanol fuel cell operating at high methanol concentrations. *Journal of Environmental Chemical Engineering*, (xxxx), 1–12. DOI: 10.1016/j.ijhydene.2020.02.101.

[33] Shangguan, Z., Li, B., Zhang, C. (2021). Understanding the functions and modi fi cations of interfaces in membrane electrode assemblies of proton exchange membrane fuel cells. *Journal of Materials Chemistry A*, 9, 15111–15139. DOI:

10.1039/d1ta01591e.